Title

Positron Emission Tomography Imaging of Functional Transforming Growth Factor β (TGFβ) Activity and Benefit of TGFβ Inhibition in Irradiated Intracranial Tumors

Journal

International Journal of Radiation Oncology • Biology • Physics, 109(2)

ISSN

0360-3016

Authors

Gonzalez-Junca, Alba

Reiners, Oliver

Borrero-Garcia, Luis D

et al.

Publication Date

2021-02-01

DOI

10.1016/j.ijrobp.2020.09.043

Peer reviewed

Positron Emission Tomography Imaging of Functional TGFβ Activity and Benefit of TGFβ Inhibition in Irradiated Intracranial Tumors

Alba Gonzalez-Junca, Ph.D[1]*; Oliver Reiners, Ph.D[1*]; Luis D. Borrero-Garcia, Ph.D[1]; Denis Beckford-Vera, Ph.D[2]; Ann A. Lazar, Ph.D[4,5,6]; William Chou, BA[1]; Steve Braunstein, MD/PhD[1], Henry VanBrocklin, Ph.D[2], Benjamin L. Franc, MD[2,3]; Mary Helen Barcellos-Hoff, Ph.D[1,4*]

[1] Department of Radiation Oncology, School of Medicine, University of California San Francisco, San Francisco, CA, USA

[2] Department of Radiology and Biomedical Imaging, University of California San Francisco, San Francisco, CA, USA

[3] Current address: Department of Radiology, Stanford University, School of Medicine, Palo Alto, CA, USA

[4] Helen Diller Family Comprehensive Cancer Center, School of Medicine, University of California San Francisco, San Francisco, CA, USA

[5] Division of Oral Epidemiology, School of Dentistry, University of California San Francisco, San Francisco, CA, USA

[6] Division of Biostatistics, School of Medicine, University of California San Francisco, San Francisco, CA, USA

* Contributed equally

Running title: Functional Imaging of TGFβ Activity

Keywords: Glioblastoma, brain metastases, TGFβ, ionizing radiation, positron emission tomography, functional imaging

Financial Support: This research was supported by Varian Medical Systems research grant, National Institutes of Health R01NS109911 and U.S. Department of Defense Congressionally Directed Medical Research Award BC160513 to MHBH, and U.S. Department of Defense Congressionally Directed Medical Research Award BC160513P1 to BLF at UCSF.

Corresponding Author:

Mary Helen Barcellos-Hoff, Ph.D.
Department of Radiation Oncology
Helen Diller Family Comprehensive Cancer Center
School of Medicine

University of California, San Francisco
2340 Sutter St., San Francisco, CA 94143
(415) 476-8091
MaryHelen.Barcellos-Hoff@ucsf.edu

Statistical analysis:

Ann A. Lazar, Ph.D.
Division of Oral Epidemiology
School of Medicine
University of California. San Francisco
Ann.Lazar@ucsf.edu

Conflicts of Interest: The authors declare there are no conflicts of interest regarding these data.

Data sharing statement: Research data are stored in an institutional repository and will be shared upon request to the corresponding author.

Author Contribution or Task: AGJ, OR, LBG, and WC conducted experimental studies; AGJ and OR analyzed data and prepared the data for publication; AL analyzed data; DBV and HVB conducted radiochemistry and image analysis; SB, BF and MHBH designed study; AGJ, OR, BF and MHBH wrote manuscript; all authors revised and approved final manuscript.

Word count: 7790

References: 52

Figures: 4

Tables: 0

Supplementary Figures: 3

Supplementary Tables: 0

Acknowledgements: The authors wish to thank Mr. Trevor Jones and Ms. Hui Zhang for expert technical assistance. These studies were supported by awards to MHBH from Varian Medical Systems, Inc., NIH R01NS109911, and DOD-BCRP W81XWH-17-1-0032, and to BF from DOD-BCRP W81XWH-17-1-0033.

ABSTRACT

Introduction: Transforming growth factor β (TGFβ) promotes cell survival by endorsing DNA damage repair and mediates an immunosuppressive tumor microenvironment. Thus, TGFβ activation in response to radiation therapy is potentially targetable because it opposes therapeutic control. Strategies to assess this potential in the clinic are needed.

Methods & Materials: We evaluated positron emission tomography (PET) to image ^{89}Zr -fresolimumab, a humanized TGFβ neutralizing monoclonal antibody, as means to detect TGFβ activation in intracranial tumor models. TGFβ pathway activity was validated by immunodetection of phosphorylated SMAD2 and TGFβ target, tenascin. The contribution of TGFβ to radiation response was assessed by Kaplan Meier survival analysis of mice bearing intracranial murine tumor models, GL261 and SB28 glioblastoma and brain-adapted 4T1 breast cancer (4T1-BrA) treated with TGFβ neutralizing monoclonal antibody, 1D11, and/or focal radiation (10 Gy).

Results: ^{89}Zr-fresolimumab PET imaging detected engineered, physiological and radiation-induced TGFβ activation, which was confirmed by immunostaining of biological markers. GL261 glioblastoma tumors had more PET signal compared to similar sized SB28 glioblastoma tumors, whereas widespread PET signal of 4T1-BrA intracranial tumors is consistent with its highly dispersed histological distribution. Survival of mice bearing intracranial tumors treated with 1D11 neutralizing antibody alone was similar to that of mice treated with control antibody whereas 1D11 improved survival when given in combination with focal radiation. The extent of survival benefit of combination of radiation and 1D11 was associated with the degree of TGFβ activity detected by PET.

Conclusions: This study demonstrates that ^{89}Zr -fresolimumab PET imaging detects radiation-induced TGFβ activation in tumors. Functional imaging indicated a range of TGFβ activity in intracranial tumors, but TGFβ blockade provided survival benefit only in the context of radiation treatment. These studies are further evidence that radiation-induced TGFβ activity opposes therapeutic response to radiation.

INTRODUCTION

Transforming growth factor β (TGFβ) is a critical regulator of the tumor microenvironment (TME). It mediates extracellular matrix (ECM) remodeling, angiogenesis and immunosuppression, and regulates tumor cell motility and invasion (1). Elevated plasma TGFβ correlates with poor outcome for breast, lung and hepatocellular carcinoma patients (reviewed in (2)). Of particular clinical significance is the role of TGFβ in glioblastoma (GBM) in which increased TGFβ signaling is associated with poor prognosis (3) and recurrent GBMs exhibit increased mRNA for *TGFB1*, its receptors and its direct target, tenascin C (TNC), and activation of signaling evidenced by SMAD phosphorylation (4). Genomic analysis of recurrent GBM found that about 11% of all tumors harbor a *de novo* mutation that further increases TGFβ activity (5), suggestive of a strong selective pressure from TGFβ during tumor recurrence.

Inhibition of TGFβ sensitizes cancer cells and tumors to radiation treatment (RT). GBM and lung cancer cell lines were treated with the small molecule inhibitor blocking TGFβ type 1 receptor kinase. The small molecule restored radiation sensitivity and decreased cancer stem cell resistance. Mice bearing subcutaneous breast or lung tumors were injected with 1D11, a pan-isoform TGFβ neutralizing antibody. Both models showed increased radiosensitivity and decreased tumor growth when treated with 1D11 before radiation (6-8). A second small molecule inhibiting TGFβR1, LY210761, was tested in orthotopic xenografts and cell culture models. In line with LY364947 and 1D11, it increased radiosensitivity of GBM cells. Furthermore, it increased survival of nude mice bearing brain tumors independent of radiation (9,10). Besides dampening of radiation-induced damage, TGFβ is known to remodel the TME and suppress the immune system. Taken together TGFβ signaling promotes malignant phenotypes that might contribute to failure of tumor control (reviewed in (11)). Thus, the clinical motivation for targeting TGFβ inhibition in cancer and RT is high.

TGFβ activation is controlled by its production as a latent complex which is bound to the latency associated peptide (LAP) (12). The latent TGFβ complex is secreted, often in association with binding proteins that sequester the complex in the ECM. Extracellular or pericellular activation of latent to functional TGFβ can be triggered by changes in pH, reactive oxygen species, mechanical stress, or enzymatic cleavage, and is required for effective functional binding to its ubiquitous receptors. TGFβ activation is essential to initiate signaling and subsequent pathway stimulation, but it is difficult to monitor when and where functional TGFβ contributes to cancer biology, which obscures its potential as a therapeutic target.

Here we radiolabeled fresolimumab, a humanized form of TGFβ neutralizing monoclonal 1D11, with ^{89}Zr for positron emission tomography (PET) imaging TGFβ activity in murine tumors. As reported (13),

^{89}Zr -fresolimumab fully preserved immunoreactivity. We used genetically engineered, physiological and irradiated tumor models to demonstrate that ^{89}Zr -fresolimumab PET specifically detects active TGFβ, which was validated by immunostaining of TGFβ pathway and targets. Functional imaging demonstrated prominent TGFβ activation in GL261 and SB28 GBM intracranial tumors and an 4T1 breast cancer intracranial model of brain metastases. Treatment of mice bearing intracranial tumors with TGFβ neutralizing antibody had no effect on tumor control but reduced TGFβ biological targets and significantly improved tumor control of irradiated tumors in all models. Together these studies demonstrate the feasibility of functional monitoring of TGFβ activity and the potential benefit of its targeting in combination with RT.

MATERIAL & METHODS

Cell lines

Cell lines were authenticated and routinely assayed to confirm that they were free of mycoplasma. GL261-luciferase (GL261) cell line provided by Dr. Nalin Gupta (UCSF) were cultured in Dulbecco's modified Eagle's medium (DMEM) and 10% fetal bovine serum (FBS). SB28-luciferase cell line (SB28), generated using sleeping beauty transposon system (14), provided by Dr. Hideho Okada (UCSF) were cultured with Roswell Park Memorial Institute medium (RPMI 1640), supplemented with 10% FBS (HyClone), GlutaMax (Thermo Fisher), 1 mM Sodium Pyruvate and 1% MEM non-essential amino acids (MEM NEAA 100X, Thermo Fisher). Lewis lung carcinoma (LLC) cells transfected with the integrin αvβ8 (β8 LLC) and control vector provided from Dr. Stephen L. Nishimura (UCSF) were cultured in DMEM supplemented with 10% FBS and 1 mg/mL geneticin. Human 293 renal sarcoma cell line clone C19 transfected with TGFβ expression plasmid in which site-directed mutagenesis of two cysteine codons to serine codons results in constitutively active TGFβ and clone B9 overexpresses wild type latent TGFβ1 (15) were cultured with DMEM and 5% FBS. BALB/c murine breast cancer cell line 4T1-luciferase-mCherry was obtained from Dr. David Lyden (Weil-Cornel Medical School). To create a model of brain metastases, 4T1-luc-mCherry cells were inoculated intracranially into BALB/c female mice and mCherry^{+} tumor cells were sorted from resulting tumors. The brain-adapted cells were pooled and expanded to generate the cell line designated 4T1-BrA, which was authenticated and confirmed mycoplasma free. Cells were cultured in DMEM containing 10% FBS and expanded *in vitro* for 2 passages prior to viable freezing in aliquots for subsequent animal inoculation.

Tumor models and treatment

For intracranial tumors, a stereotaxic device was used to inject cells 1 mm anterior and 1.8 mm lateral of the bregma in the right brain hemisphere and 3.5 mm beneath the skull surface into the corpus striatum

of 6–7 week old syngeneic mice anesthetized with ketamine/xylazine (90 mg/kg) and buprenorphine (0.5 mg/kg) whilst maintaining body temperature. SB28 ($5x10^4$) or GL261 (10^5) cells were injected into C57BL/6J mice and 4T1-BrA cells ($3x10^3$) were injected into BALB/cJ female mice. Intracranial tumor growth was measured by bioluminescence (BLI) imaged (Xenogen IVIS 100 Imaging System) every 5 days following intraperitoneal (i.p.) injection of 200 µl (15 mg/mL) luciferin under anesthesia using 2% isoflurane. Tumor burden was calculated based on bioluminescence flux (photons/sec) and was used to randomize mice to treatment groups as follows: Sham IgG, Sham 1D11, RT+IgG, or RT+ID11. TGFβ neutralizing antibody 1D11 (25 mg/kg, i.p., 3x week, up to 4 weeks, Bioxcell, BP0057) or IgG control antibody (25 mg/kg, i.p., 3x week, up to 4 weeks, Bioxcell, BP0083) was administered 24 h before irradiation with 10 Gy using small animal radiation research platform (SARRP, XStrahl) individualized plans (Muriplan, XStrahl) based on arc beam computerized tomography (CT). Mice bearing intracranial tumors were monitored for neurological symptoms or weight loss (≥ 15% body weight) and sacrificed in accord with the UCSF Institutional Animal Care and Use Committee guidelines.

For subcutaneous tumors, 4T1-BrA (10^5) cells were injected into the flanks of BALB/cJ female mice, human renal cell sarcoma B9 or C19 ($5x10^6$) cells were injected into flanks of BALB/c Foxn1/nu mice, and LLC and β8 LLC ($2x10^6$) cells were injected into the flanks of C57BL/6J mice. In some studies, subcutaneous tumors were irradiated under anesthesia using 2% isoflurane with 15 Gy using the SARRP.

Preparation and validation of the ^{89}Zr-fresolimumab imaging probe

For radiolabeling, 20 mg of fresolimumab (kindly provided by Genzyme, Inc.) in 1 mL of 0.1 M sodium carbonate solution (pH 9) was mixed with 3-fold molar excess of DFO-p-SCN (Macrocyclics, Inc., Plano TX) previously dissolved in 20 µL of anhydrous DMSO. The reaction mixture was incubated for 45 min at 37 °C with gentle stirring. The DFO-fresolimumab conjugate was purified by size-exclusion chromatography using a PD-10 column. Fractions containing DFO-fresolimumab were pooled and concentrated via ultracentrifugation using an Amicon filter device (30 MWCO). DFO-fresolimumab conjugate was characterized by size-exclusion High Performance Liquid Chromatography (SE-HPLC) (Supplementary Fig. 1). Protein concentration was determined by Bradford spectrophotometric assay. The average number of chelates linked to an antibody molecule was determined by isotopic dilution assay, as previously described (16), using ^{89}Zr spiked with a known amount of $ZrCl_4$.

For radiolabeling, 10 µL (130 MBq/ 3.5 mCi) of ^{89}Zr-Oxolate (3D Imaging LLC, Little Rock AR) and 10 µL of 1M Na_2CO_3 were added to 20 µL of water, and allowed to stand for 3 min. Subsequently 200 µL of 1M ammonium acetate and 100 µg of DFO-fresolimumab (16 mg/mL in PBS), were added to the vial containing neutralized ^{89}Zr and the reaction mixture was incubated for 1h at room temperature. Radiolabeled conjugate was purified from unbound radiometal by size exclusion using a PD-10 desalting

column with 0.9% NaCl as the eluent. Fractions (1 mL) were collected, and radioactivity was measured. Radiolabeling yield was calculated from the ratio of activity in the fractions containing ^{89}Zr-DFO-fresolimumab (^{89}Zr-fresolimumab) to the initial activity used for the radiolabeling. Chemical and radiochemical purity was determined by SE-HPLC and iTLC.

To assay binding competition, a 96 well microtiter plate was coated with recombinant human TGFβ 3 (100 µL, 4 µg/mL in PBS) overnight at 4 °C. The following day, the solution in each well was discarded and wells were washed three times with 0.5% Tween in PBS. A solution of 1% nonfat milk (150 µL) was added to each well and the microtiter plate was blocked at room temperature for 1 h. Afterwards, the solution in each well was discarded. Solutions containing equal amount of ^{89}Zr-fresolimumab (100 µL, 20 MBq) and increasing amount of unmodified ("cold") fresolimumab (0.08 to 92 nM) were added to the microtiter plate and incubated for 1 h at room temperature. The solution in each well was discarded and wells were washed three times with 0.5% Tween in PBS. Sodium hydroxide (NaOH) solution (1 M, 200 µL) was added to each well and incubated for 20 min. The NaOH solution in each well was pipetted into test tubes and the radioactivity was measured using a HIDEX automated gamma counter (Turku, Finland). Concentration values that caused 50% of inhibition (IC50) of ^{89}Zr-fresolimumab to recombinant human TGFβ 3 were estimated from the non-linear fitted curves using GraphPad Prism (GraphPad Software, Inc., San Diego, CA) (Supplementary Fig. 1).

In vivo PET/CT imaging

Mice were injected i.p. with a dose of 140 – 150 µCi ^{89}Zr-fresolimumab or 200 µCi ^{18}F-flurodeoxyglucose (FDG). At various times following injection, mice were anesthetized with inhaled 2% isoflurane and imaged under isoflurane and body temperature maintenance using a pre-clinical PET/CT scanner (GNEXT PET/CT, SOFIE Inc.). In some experiments, (Fig. 2D), half of the mice harboring subcutaneous 4T1-BrA tumors were injected with unlabeled (cold) fresolimumab 24 h prior to radioactive-fresolimumab injection. At 96 h after injection, mice were euthanized and tumors were collected to calculate the percentage of injected dose per gram (%ID/g) based on radioactive counts in harvested tissues measured by the HIDEX automated gamma counter (17).

Mice with subcutaneous tumors were imaged 96 h after ^{89}Zr-fresolimumab injection and mice with intracranial tumors were imaged 24 h after to 120 h after ^{89}Zr-fresolimumab injection. In some experiments, mice were injected with ^{18}F-fluorodeoxyglucose (^{18}F-FDG) and imaged 30 min after injection. PET scans were 10 minutes each. Images were reconstructed using 3D-OSEM with an energy window of 350-650 keV. CT scans were 1 minute each with 720 projections acquired over 360 degrees. CT images were reconstructed using a modified Feldkamp method. Analysis of PET/CT was performed using AMIDE (Amide Medical Imaging Data Examiner) (18). Volumes of interest were drawn and the uptake (Bq/mL)

calculated. Image data were corrected for attenuation, decay and volume, and displayed as percentage of injected dose per mL (% ID/mL). Representative images are projections of multiple slices represent the whole mouse / mouse head. All pictures shown use the same display settings in AMIDE.

Immunostaining

Tumor bearing brains were collected at 5 days post radiation for TGFβ marker analysis. Harvested tissues were fixed in a 10% buffered formalin phosphate solution. After 24 h, brains were transferred into a 70% ethanol solution and embedded in paraffin (FFPE). Sections (3 µm) were subjected to acidic antigen retrieval (Antigen Unmasking Solution, Citric Acid Based, Vector, H-3300) followed by blocking with the supernatant of 0.5% casein (Spectrum, CA205) stirred for 1 hr in PBS. Sections were incubated with mouse monoclonal antibody against TGFβ (Bioxcell, BP0057, mouse), against pSMAD2 (Cell Signaling #3108, rabbit) or TNC (Abcam, #AB108930, rabbit) at 4 °C overnight. The next day, slides were incubated for 1 h with fluorochrome-labeled secondary antibodies against rabbit (Alexa-fluor595, Life Technologies, #A21207 or Alexa-fluor488, Life Technologies, #A21206) or mouse (Alexa-fluor488, Life Technologies, #A21202) and counterstained with 4,6-diamidino-2-phenylindol (DAPI, Thermo Fisher, #D1306) for nuclear content. Sections were washed and mounted with Vectashield (Vector Labs, H1000) and stored at -25 °C in the dark. Slides were imaged with a Zeiss Axiovert epifluorescence microscope and at least five representative fields of interest were analyzed with ImageJ (19). Fluorescence intensity of different markers relative to field or amount of positive stained nuclei were calculated and reported as arbitrary units (AU). Shown data points depict the average of all taken representative pictures.

Statistical Method

In each experiment, mice were randomized to one of the four treatments. Descriptive statistics were used to summarize the data, for continuous variables, means and standard deviations (SD), and for categorical variables, frequencies, and percent. N represents the number of animals per group. For continuous variables with matched groups, paired t-test was used, and for independent groups, analysis of variance was used with adjustment of alpha level for multiple testing using Bonferroni correction for post-hoc pairwise t-tests. Overall survival was calculated using Kaplan–Meier. Log-rank test was used to compare groups. Two-sided p-values less than 0.05 were considered statistically significant. SAS v. 9.4 software was used to perform the analyses.

RESULTS

^{89}Zr-fresolimumab specifically detects active TGFβ in engineered tumor models

To ascertain the specificity of functional imaging of fresolimumab, the humanized version of murine pan-isoform TGFβ neutralizing antibody 1D11, it was radiolabeled with ^{89}Zr using DFO conjugation (Supplementary Fig. 1A). ^{89}Zr-fresolimumab yield, radiochemical purity and biological activity were determined after conjugation and radiolabeling (Supplementary Fig. 1 B - D).

To determine if PET imaging of ^{89}Zr-fresolimumab can effectively discriminate between active and latent TGFβ, we established tumors from human tumor cell line, B9, which is stably transfected with a construct to overexpress wild-type latent TGFβ1, and isogenic C19 cell line, which expresses constitutively active TGFβ1 (15,20). Mice bearing contralateral flank tumors of each cell line were imaged by PET and computerized tomography (CT). ^{89}Zr -fresolimumab PET imaging showed greater signal in the C19 tumors, compared to the contralateral B9 tumors, which exhibited minimal PET signal (Fig. 1A). Analysis of the percentage of injected dose (ID) present in tumors 96 h after injection confirmed a significantly greater uptake of ^{89}Zr -fresolimumab in C19 tumors (Fig. 1B). Activation of TGFβ results in signaling via receptor-mediated phosphorylation of SMAD2, which ultimately mediates expression of TGFβ gene targets (21). To validate differential TGFβ activation, we used tumor sections for immunofluorescence staining using an antibody that specifically detects active TGFβ (22) and phosphorylated SMAD2 (pSMAD2). Consistent with constitutive TGFβ activation, the amount of TGFβ immunofluorescence of C19 tumors was 5-fold greater than B9 tumors, and the percentage of pSMAD2 positive cells increased from 2% to 15% ($P < 0.05$) (Fig. 1C).

Next, we assessed whether ^{89}Zr -fresolimumab PET imaging could detect physiological activation of TGFβ in Lewis lung cell carcinoma (LLC) flank tumors. One physiological mechanism of TGFβ activation occurs at the cell surface αvβ8 integrin binds the RGD sequences in LAP of latent TGFβ 1 and 3 (23). Parental LLC that do not express the αvβ8 integrin whereas β8 LLC cells have been stably transfected to express αvβ8 (24). Mice bearing contralateral tumors obtained from LLC and β8 LLC cell subcutaneous injection were imaged using PET ^{89}Zr -fresolimumab (Fig. 1D). β8 LLC tumors exhibit more radioactivity compared to uptake of the contralateral parental LLC tumor (Fig. 1E). Immunostaining of tumor sections confirmed significantly greater active TGFβ ($p<0.05$) as well as an increased frequency of pSMAD2 cells from 2% to 14% ($P < 0.05$) in β8 LLC tumors (Fig. 1F).

^{89}Zr-fresolimumab detects radiation-induced TGFβ activity

Radiation elicits rapid and sustained TGFβ activation activity (25), that may occur due to a redox susceptible reduction of a methionine in TGFβ1 LAP (26). We next sought to determine if ^{89}Zr -

fresolimumab PET imaging would detect more TGFβ activity in irradiated tumors. Mice were injected subcutaneously with 4T1-BrA cells in both flanks to establish bilateral tumors. The right tumor was irradiated with 15 Gy using a small animal radiation research platform and mice were injected with ^{89}Zr -fresolimumab 24 h before RT. Mice were imaged with PET 96 h later. Irradiated tumors displayed significantly increased PET signal relative to non-irradiated contralateral tumors (Fig. 2A). Radioactivity was subsequently quantified *ex vivo* by autoradiography or gamma counting. Autoradiograms of tumor sections confirmed that the irradiated tumors were more radioactive than contralateral non-irradiated tumors (Fig. 2B). Irradiated tumors also contained more radioactive isotope compared to contralateral tumors (Fig. 2C). The specificity of ^{89}Zr -fresolimumab was assessed by injecting 4T1-BrA tumor bearing mice with unlabeled fresolimumab prior to radioactive-fresolimumab to block target antigen. As expected, the activity per gram of tissue was decreased in mice that were administered unlabeled fresolimumab (Fig. 2D).

Immunostaining of tumor sections indicated that active TGFβ and pSMAD2 positive cells increased in irradiated compared to non-irradiated tumors (Fig. 2E). The frequency of pSMAD2 positive cells per field significantly increased ($P < 0.05$) from 15% to 22% after radiation (Fig. 2F). We next examined TNC, which is induced by TGFβ (27). Irradiated tumors showed significantly increased TNC (Fig. 2G), as quantified by image analysis (Fig. 2H). These markers confirm the expected biological consequences of radiation-induced activation of TGFβ and its downstream signaling. Together, these data confirms that ^{89}Zr-fresolimumab PET detects active TGFβ in multiple contexts.

Imaging TGFβ activity in murine intracranial tumors

Brain tumors are highly aggressive and retrospective analysis of TGFβ activity suggests that it might be important in patient response (3)Bayin, 2016 #21059]. Due to the intracranial location and the rapid course of the disease, a non-invasive means to detect TGFβ activity could be of clinical utility. Here, we used two orthotopic glioblastoma models, SB28 and GL261, and 4T1-BrA intracranial breast cancer model of brain metastases bearing luciferase reporters. Mice receiving sham surgery injected intracranially with PBS were used as control (Supplemental Fig. 2A). Intracranial SB28 (Fig. 3A), GL261 (Fig. 3B) and 4T1-BrA (Fig. 3C) tumors confirmed by BLI. were imaged with^{89}Zr-fresolimumab PET. Signal quantification in SB28 tumors imaged 96 h after injection was significantly greater in tumor-bearing brains compared to sham surgery (Fig. 3D). GL261 tumors exhibited twice as much ^{89}Zr-fresolimumab PET signal compared to SB28 tumors that appeared comparable by BLI (Fig. 3E, Supplemental Fig. 2B).

Imaging invasive brain metastases may be affected by presence of multiple extra-cranial metastases. To model this clinical presentation, we injected mice with intracranial and subcutaneous tumors and imaged with ^{89}Zr-fresolimumab PET (Fig. 3F). Signal was detected in both brain and flank tumors indicating that

functional monitoring of multiple sites is possible. These data show that functional imaging of TGFβ activity in intracranial tumors as well as extracranial tumor locations is feasible.

TGFβ neutralizing antibody inhibits TGFβ signaling in intracranial tumors

Given the evidence of intracranial functional imaging using fresolimumab, we investigated whether TGFβ could be functionally blocked by 1D11, the murine monoclonal TGFβ neutralizing antibody on which fresolimumab is based, in the context of with focal (i.e. to BLI defined volume) radiation treatment. Histological analysis of tumors at termination demonstrated that SB28 and 4T1-BrA tumors were highly invasive morphology compared to localized GL261 tumor (Supplemental Fig. 2E-G). In some mice SB28 tumors were found to have traversed the corpus callosum to the contralateral hemisphere at termination. 1D11 or a control antibody was administered i.p. one day before RT with 10 Gy. To evaluate 1D11 efficacy, tumors were harvested 5 days later for pSMAD2 and TNC immunostaining (Supplemental Fig. 2C, D).

The frequency of pSMAD2 positive cells was low in all tumor models in sham-irradiated mice treated with control antibody, which was unaffected by 1D11 treatment, in SB28 (Fig. 4A), GL261 (Fig. 4B), and 4T1-BrA (Fig. 4C) tumors. The frequency of pSMAD2 positive cells significantly increased in all irradiated tumors, which was prevented by treatment with 1D11 neutralizing antibody. Consistent with TGFβ signaling, TNC was increased in irradiated SB28 (Fig. 4D), GL261 (Fig. 4E), and 4T1-BrA (Fig. 4F) tumors and treatment with 1D11 effectively decreased TNC after RT. Although the radiation-induced change in pSMAD2 was similar in each tumor model, the amount of TNC deposition in the irradiated TME was greater in GL261 compared to either SB28 or 4T1-BrA. Together, these results show that radiation induced TGFβ signaling can be effectively inhibited by concomitant treatment with the neutralizing antibody 1D11, as evidenced by changes in pathway activity and ECM remodeling, indicating that the blood-brain barriers to the gross volume of tumor is compromised.

TGFβ blockade in combination with RT increases survival in brain cancer models

Based on functional imaging and biological response, we confirmed that TGFβ activity is increased in irradiated brain tumors, thus we investigated the therapeutic response to TGFβ inhibition in these models. Administration of 1D11 had no effect on tumor growth in these model as evidenced by BLI (Supplemental Fig. 3) or survival (Fig. 4 G-I), except for a single long-term survivor of a GL261 tumor bearing mouse. For mice bearing SB28 tumors, RT provided modest increase in median survival (21 days) compared to sham (19 days), whereas RT+1D11 combination treatment significantly (P<0.05) increased median survival to 31 days (Fig. 4G). For mice bearing intracranial GL261 tumors, RT significantly (P<0.05) improved survival from 17 to 30 days (Fig. 4H). The combination of RT and 1D11 treatment significantly (P<0.01) prolonged survival but median survival not reached because 80% of mice exhibited long term

tumor-free survival. Long-term survivors lacked evidence of tumor as evidenced by BLI (Supplemental Fig. 3B). In 4T1-BrA intracranial tumors, RT significantly (P<0.0001) increased median survival from 17 to 33 days and resulted in 3 out of 12 (25%) long term survivors (Fig. 4I). Treatment with 1D11+RT significantly (P<0.0001) increased survival to 41 days and 4 out of 13 (30%) mice had a durable response. Hence, radiation-induced TGFβ is a biological target that mediates tumor response to radiation.

DISCUSSION

A vast literature on TGFβ signaling in cancer indicates that it is key to many aspects of tumor biology, including growth control, cancer stem cell self-renewal, vascularity, extracellular matrix composition and immune infiltration. Moreover, TGFβ is a widely distributed and broadly active in across cancers, which is associated with poor prognosis (reviewed in (28)). Extracellular TGFβ activation is essential to initiate signaling and subsequent pathway stimulation, but lack of tools to determine when and where functional TGFβ occurs obscures its potential as a therapeutic target. Here we set out to refine ^{89}Zr-fresolimumab PET imaging (13). Prior studies with functional TGFβ imaging lacked evidence that fresolimumab differentiates between latent and active TGFβ. To do so, we used tumor models in which TGFβ activation had been genetically engineered, physiologically activated, or radiation induced. In each case, ^{89}Zr-fresolimumab PET discriminated between tumors with greater or lesser TGFβ activation as determined by immunostaining of phosphorylated SMAD2, active TGFβ and target protein, TNC deposition. Prior reports of increased ^{89}Zr-fresolimumab PET in recurrent GBM (29) and the prominent role of TGFβ in this intractable disease (3,4), led us to extended explicit functional validation to clinically relevant tumor models of intracranial GBM and breast cancer metastases and to test its biological relevance in the context of RT. ^{89}Zr-fresolimumab PET functional imaging of intracranial tumors demonstrated prominent TGFβ activation and de facto antibody access, indicating that this antibody crosses the leaky GBM blood brain barrier, like standard of care bevacizumab (30). Moreover, treatment with TGFβ blocking antibody, which lacked tumor control efficacy on its own, was effective in blocking TGFβ signaling and significantly improved response to RT in each model.

Over the last decade, multiple mechanisms by which TGFβ signaling affects responses to RT have come to light. Therapeutic control is determined by the degree and type of DNA damage inflicted and the cellular capacity to repair the damage. Successful repair requires the ability to recognize DNA damage, assemble the repair machinery, and execute repair; abrogation of any of these components decreases cell survival. Inhibition of TGFβ signaling leads to reduced phosphorylation of critical DNA damage transducers, abrogation of the cell cycle checkpoint and increased radiosensitivity (31,32). The requirement for TGFβ in the genotoxic stress program provoked translational studies in breast, brain and lung cancer models treated with either TGFβ neutralizing antibodies or small molecule inhibitors of TGFβ signaling in

the context of radiation. Decreased DNA damage recognition and ineffective cell cycle arrest are accompanied by greater radiation sensitivity. Treating breast, brain, oropharyngeal and lung cancer cell lines with a small molecule inhibitor of the TGFβ type I receptor I kinase activity prior to radiation exposure substantially decreases (10-70%) dose needed to reduce survival to 10% as measured by clonogenic cell survival in most (35/43) cell lines that we have tested (6-8,33). Irradiation of tumors in mice treated with preclinical pan-neutralizing TGFβ antibodies exhibit defective DNA damage recognition and increased tumor control (6-8).

The response of tumors to radiation also depends on host cells within the TME, particularly vasculature and immune cells (34). TGFβ neutralizing antibodies not only promotes response to fractionated radiation in breast cancer preclinical models but also augments response to checkpoint inhibition (35). We noted that 1D11 and RT resulted in long-term tumor-free survival in 80% of mice bearing GL261 and about 30% of the mice bearing 4T1-BrA intracranial tumors. This durable control is provocative as TGFβ is an important determinant of immune cell phenotypes. We showed that irradiated breast cancer cells co-cultured with monocyte precursors increase differentiation of myeloid derived suppressor cells (MDSC), which TGFβ mediates by both increasing immature monocyte survival and driving profoundly immunosuppressive phenotypes (36). TGFβ induced MDSC promote the differentiation of CD4+ T cells towards Treg. MDSC can suppress cytotoxic T-cell activation and proliferation by depleting arginine through the expression of arginase-1, increasing nitric oxide levels through iNOS expression and by secreting immunosuppressive cytokines, including TGFβ and IL-10 (36-39). MDSC are prominent in GBM and associated with poor prognosis (40).

Radiation elicited persistent TGFβ activation that mediated remodeling of the TME in preclinical models of brain tumors. TNC, an ECM glycoprotein, is highly expressed in gliomas where it appears to play a critical role in cell migration and invasion (41). Administration of neutralizing antibody, 1D11, blocked radiation-induced TNC deposition. Notably, TNC is associated with ECM stiffness, measured by atomic force microscopy, which is greater in GBM compared to low grade gliomas (42). To test whether TNC contributes to GBM biology, TNC was knocked down in a GBM xenograft model. Tumors in which TNC was inhibited were softer, had markedly reduced focal adhesion signaling, grew more slowly, were smaller and less vascularized; consequently, the mice survived almost twice as long as compared to mice injected with control tumor cells (43).

Strategies to block the signaling of TGFβ include kinase inhibitors, neutralizing antibodies and protein traps have been tested in early phase clinical trials (reviewed in (44). Each as potential clinical advantages. Small molecules are thought to have greater access, whereas biologics are thought to be limited in some situations, like the brain, due to their molecular weight and glycosylation. On the other hand, antibody

stability and longer half-life can be beneficial. Galusertinib (LY2157299), a pyrazole derivative, showed promising activity in GBM by reducing glioma initiating cells (45,46). Phase 1 clinical trials in glioma and advanced cancer showed feasibility (47), but combination with lomustine in recurrent GBM failed to demonstrate benefit (48,49). Fresolimumab is based on the TGFβ neutralizing murine monoclonal antibody1D11, which augments radiation response in multiple preclinical models (11). Phase 1 studies in melanoma and renal cell carcinoma patients showed acceptable safety (50). Notably, fresolimumab in combination with fractionated radiation to one to three sites in metastatic breast cancer patients pointed towards survival benefit in a dose-dependent manner (51).

There are limitations to this study. TGFβ activation is notoriously difficult to ascertain in situ and there are no quantitative assays (52). Hence, we did not explicitly determine the sensitivity range and potential saturation of ^{89}Zr-fresolimumab in this study. Here we compared functional imaging based on biological TGFβ response, i.e. SMAD phosphorylation or TNC deposition, as surrogates for activation in tumor models in which TGFβ was genetically engineered for constitutive activation (i.e. B9 vs C19), or induced by integrin overexpression (i.e. LLC vs β8LLC), or irradiated. It is not known whether ^{89}Zr-fresolimumab has comparable efficiency to detect each mechanism of activation, or how sensitive it is to different TGFβ isoforms. Fresolimumab binds to all three isoforms, albeit with greater affinity for TGFB1 and B3 than for B2 (53), whereas the engineered activation is specifically that of TGFB1, and integrin activation is not possible for TGFB2 since its LAP lacks an RGD binding site. We did not examine a time course, although the 3-day radioactive half-life of ^{89}Zr-fresolimumab could feasibly be imaged up to 5 half-lives, i.e. 15 days. It is possible that antibody-based imaging could be used to select patients for treatment with a small molecule inhibitor. Lastly, only a single radiation dose was used to evaluate the effect of TGFβ inhibition on survival, whereas a comparison of radiation regimes will likely be important for extrapolation to the clinic.

We and others have shown that genotoxic cancer therapies, including radiation, cisplatin and temozolomide, elicit TGFβ activity that persists long after completion of treatment (reviewed in (1,11)). TGFβ signaling promotes a permissive TME, immunosuppression and mediates the execution of the DNA damage response; hence, TGFβ in cancer limits effective tumor control. Despite abundant evidence that TGFβ opposes effective cancer therapy, the question of whether TGFβ signaling can be targeted to improve cancer outcomes remains open. Here, we demonstrate the specificity of ^{89}Zr-fresolimumab as a novel non-invasive molecular imaging tool to assess TGFβ activity, expanding the current spectrum for functional PET imaging of intracranial tumors. Our preclinical studies further support the concept TGFβ opposes therapeutic benefit of RT and provide additional motivation to clinically exploit mechanisms by which TGFβ mediates the tumor control in response to radiation.

REFERENCES

1. Barcellos-Hoff MH, Newcomb EW, Zagzag D, et al. Therapeutic targets in malignant glioblastoma microenvironment. *Seminars in radiation oncology* 2009 19:163-70.
2. Teicher BA. Transforming Growth Factor-β and the Immune Response to Malignant Disease. *Clinical Cancer Research* 2007;13:6247-6251.
3. Bruna A, Darken RS, Rojo F, et al. High TGFbeta-Smad activity confers poor prognosis in glioma patients and promotes cell proliferation depending on the methylation of the PDGF-B gene. *Cancer Cell* 2007;11:147-60.
4. Bayin NS, Ma L, Thomas C, et al. Patient-Specific Screening Using High-Grade Glioma Explants to Determine Potential Radiosensitization by a TGF-beta Small Molecule Inhibitor. *Neoplasia (New York, NY)* 2016;18:795-805.
5. Wang J, Cazzato E, Ladewig E, et al. Clonal evolution of glioblastoma under therapy. *Nature genetics* 2016;48:768-76.
6. Bouquet SF, Pal A, Pilones KA, et al. Transforming growth factor b1 inhibition increases the radiosensitivity of breast cancer cells *in vitro* and promotes tumor control by radiation *in vivo*. *Clin Cancer Res* 2011;17:6754-65.
7. Hardee ME, Marciscano AE, Medina-Ramirez CM, et al. Resistance of glioblastoma-initiating cells to radiation mediated by the tumor microenvironment can be abolished by inhibiting transforming growth factor-beta. *Cancer research* 2012;72:4119-29.
8. Du S, Bouquet F, Lo C-H, et al. Attenuation of the DNA Damage Response by TGFβ Inhibitors Enhances Radiation Sensitivity of NSCLC Cells In Vitro and In Vivo *Int J Radiat Oncol Biol Phys* 2014;91:91-99.
9. Zhang M, Herion TW, Timke C, et al. Trimodal Glioblastoma Treatment Consisting of Concurrent Radiotherapy, Temozolomide, and the Novel TGF-β Receptor I Kinase Inhibitor LY2109761. *Neoplasia (New York, NY)* 2011 13:537-49.
10. Zhang M, Kleber S, Rohrich M, et al. Blockade of TGF-beta signaling by the TGFbetaR-I kinase inhibitor LY2109761 enhances radiation response and prolongs survival in glioblastoma. *Cancer research* 2011;71:7155-67.
11. Du S, Barcellos-Hoff MH. Tumors as organs: biologically augmenting radiation therapy by inhibiting transforming growth factor beta activity in carcinomas. *Seminars in radiation oncology* 2013;23:242-51.
12. Lawrence DA. Identification and activation of latent transforming growth factor b. *Meth Enzym* 1991;198:327-336.
13. Oude Munnink TH, Arjaans ME, Timmer-Bosscha H, et al. PET with the 89Zr-labeled transforming growth factor-beta antibody fresolimumab in tumor models. *Journal of nuclear medicine : official publication, Society of Nuclear Medicine* 2011;52:2001-8.
14. Genoud V, Marinari E, Nikolaev SI, et al. Responsiveness to anti-PD-1 and anti-CTLA-4 immune checkpoint blockade in SB28 and GL261 mouse glioma models. *Oncoimmunology* 2018;7:e1501137.
15. Arrick BA, Lopez AR, Elfman F, et al. Altered metabolic and adhesive properties and increased tumorigenesis associated with increased expression of transforming growth b1. *J Cell Biol* 1992;118:715-726.
16. Deri MA, Ponnala S, Kozlowski P, et al. p-SCN-Bn-HOPO: A Superior Bifunctional Chelator for (89)Zr ImmunoPET. *Bioconjugate chemistry* 2015;26:2579-91.
17. Beckford-Vera DR, Gonzalez-Junca A, Janneck JS, et al. PET/CT Imaging of Human TNFalpha Using [(89)Zr]Certolizumab Pegol in a Transgenic Preclinical Model of Rheumatoid Arthritis. *Molecular imaging and biology : MIB : the official publication of the Academy of Molecular Imaging* 2019.
18. Loening AM, Gambhir SS. AMIDE: a free software tool for multimodality medical image analysis. *Molecular imaging* 2003;2:131-7.

19. Schindelin J, Arganda-Carreras I, Frise E, et al. Fiji: an open-source platform for biological-image analysis. *Nature methods* 2012;9:676-82.
20. Barcellos-Hoff MH, Ehrhart EJ, Kalia M, et al. Immunohistochemical detection of active TGF-b *in situ* using engineered tissue. *The American journal of pathology* 1995;147:1228-1237.
21. Nakao A, Imamura T, Souchelnytskyi S, et al. TGF-beta receptor-mediated signalling through Smad2, Smad3 and Smad4. *The EMBO journal* 1997;16:5353-62.
22. Ehrhart EJ, Carroll A, Segarini P, et al. Latent transforming growth factor-b activation in situ: Quantitative and functional evidence following low dose irradiation. *FASEB J* 1997;11:991-1002.
23. Sheppard D. Integrin-mediated activation of latent transforming growth factor beta. *Cancer Metastasis Rev* 2005;24:395-402.
24. Takasaka N, Seed RI, Cormier A, et al. Integrin alphavbeta8-expressing tumor cells evade host immunity by regulating TGF-beta activation in immune cells. *JCI Insight* 2018;3.
25. Barcellos-Hoff MH, Derynck R, Tsang ML-S, et al. Transforming growth factor-b activation in irradiated murine mammary gland. *J Clin Invest* 1994;93:892-899.
26. Jobling MF, Mott JD, Finnegan MT, et al. Isoform-specific activation of latent transforming growth factor beta (LTGF-beta) by reactive oxygen species. *Radiation research* 2006;166:839-48.
27. Barcellos-Hoff MH. Radiation-induced transforming growth factor b and subsequent extracellular matrix reorganization in murine mammary gland. *Cancer research* 1993;53:3880-3886.
28. Massagué J. TGF[beta] in Cancer. *Cell* 2008;134:215-230.
29. den Hollander MW, Bensch F, Glaudemans AW, et al. TGF-beta Antibody Uptake in Recurrent High-Grade Glioma Imaged with 89Zr-Fresolimumab PET. *Journal of nuclear medicine : official publication, Society of Nuclear Medicine* 2015;56:1310-4.
30. Hulper P, Schulz-Schaeffer W, Dullin C, et al. Tumor localization of an anti-TGF-beta antibody and its effects on gliomas. *International journal of oncology* 2011;38:51-9.
31. Ewan KB, Henshall-Powell RL, Ravani SA, et al. Transforming growth factor-b1 mediates cellular response to DNA damage in situ. *Cancer research* 2002;62:5627-5631.
32. Kirshner J, Jobling MF, Pajares MJ, et al. Inhibition of transforming growth factor-beta1 signaling attenuates ataxia telangiectasia mutated activity in response to genotoxic stress. *Cancer research* 2006;66:10861-9.
33. Liu Q, Ma L, Jones T, et al. Subjugation of TGFb Signaling by Human Papilloma Virus in Head and Neck Squamous Cell Carcinoma Shifts DNA Repair from Homologous Recombination to Alternative End Joining. *Clin Cancer Res* 2018;24:6001-6014.
34. Russell JS, Brown JM. The irradiated tumor microenvironment: role of tumor-associated macrophages in vascular recovery. *Front Physiol* 2013;4:157.
35. Vanpouille-Box C, Diamond J, Pilones KA, et al. Transforming growth factor (TGF) β is a master regulator of radiotherapy-induced anti-tumor immunity. *Cancer research* 2015;75:2232-42.
36. Gonzalez-Junca A, Driscoll KE, Pellicciotta I, et al. Autocrine TGFbeta Is a Survival Factor for Monocytes and Drives Immunosuppressive Lineage Commitment. *Cancer immunology research* 2019;7:306-320.
37. Wang T, Niu G, Kortylewski M, et al. Regulation of the innate and adaptive immune responses by Stat-3 signaling in tumor cells. *Nature medicine* 2004;10:48-54.
38. Gabrilovich DI, Nagaraj S. Myeloid-derived suppressor cells as regulators of the immune system. *Nat Rev Immunol* 2009;9:162-74.
39. Marigo I, Dolcetti L, Serafini P, et al. Tumor-induced tolerance and immune suppression by myeloid derived suppressor cells. *Immunol Rev* 2008;222:162-79.
40. Kohanbash G, Okada H. Myeloid-derived suppressor cells (MDSCs) in gliomas and glioma-development. *Immunological investigations* 2012;41:658-79.
41. Brosicke N, Faissner A. Role of tenascins in the ECM of gliomas. *Cell adhesion & migration* 2015;9:131-40.

42. Laklai H, Miroshnikova YA, Pickup MW, et al. Genotype tunes pancreatic ductal adenocarcinoma tissue tension to induce matricellular fibrosis and tumor progression. *Nature medicine* 2016;22:497-505.
43. Miroshnikova YA, Mouw JK, Barnes JM, et al. Tissue mechanics promote IDH1-dependent HIF1alpha-tenascin C feedback to regulate glioblastoma aggression. *Nat Cell Biol* 2016;18:1336-1345.
44. Akhurst RJ, Hata A. Targeting the TGFbeta signalling pathway in disease. *Nat Rev Drug Discov* 2012;11:790-811.
45. Peñuelas S, Anido J, Prieto-Sánchez RM, et al. TGF-[beta] Increases Glioma-Initiating Cell Self-Renewal through the Induction of LIF in Human Glioblastoma. *Cancer Cell* 2009;15:315-327.
46. Anido J, Saez-Borderias A, Gonzalez-Junca A, et al. TGF-beta Receptor Inhibitors Target the CD44(high)/Id1(high) Glioma-Initiating Cell Population in Human Glioblastoma. *Cancer Cell* 2010;18:655-68.
47. Rodon J, Carducci M, Sepulveda-Sanchez JM, et al. Pharmacokinetic, pharmacodynamic and biomarker evaluation of transforming growth factor-beta receptor I kinase inhibitor, galunisertib, in phase 1 study in patients with advanced cancer. *Invest New Drugs* 2014.
48. Brandes AA, Carpentier AF, Kesari S, et al. A Phase II randomized study of galunisertib monotherapy or galunisertib plus lomustine compared with lomustine monotherapy in patients with recurrent glioblastoma. *Neuro-oncology* 2016;18:1146-56.
49. Capper D, von Deimling A, Brandes AA, et al. Biomarker and Histopathology Evaluation of Patients with Recurrent Glioblastoma Treated with Galunisertib, Lomustine, or the Combination of Galunisertib and Lomustine. *International journal of molecular sciences* 2017;18.
50. Morris JC, Tan AR, Olencki TE, et al. Phase I study of GC1008 (fresolimumab): a human anti-transforming growth factor-beta (TGFbeta) monoclonal antibody in patients with advanced malignant melanoma or renal cell carcinoma. *PloS one* 2014;9:e90353.
51. Formenti SC, Lee P, Adams S, et al. Focal Irradiation and Systemic TGFbeta Blockade in Metastatic Breast Cancer. *Clin Cancer Res* 2018;24:2493-2504.
52. Flanders KC, Yang YA, Herrmann M, et al. Quantitation of TGF-beta proteins in mouse tissues shows reciprocal changes in TGF-beta1 and TGF-beta3 in normal vs neoplastic mammary epithelium. *Oncotarget* 2016;7:38164-38179.
53. Bedinger D, Lao L, Khan S, et al. Development and characterization of human monoclonal antibodies that neutralize multiple TGFβ isoforms. *MAbs* 2016;8:389-404.

FIGURES & LEGENDS

Fig. 1: PET imaging of ^{89}Zr-fresolimumab detects active TGFβ *in vivo*. (A) Cartoon of mice bearing latent TGFβ producing B9 tumors (indicated by orange arrow) and active TGFβ producing C19 tumors (indicated by green arrow) and PET/CT imaging of ^{89}Zr-fresolimumab. Representative PET/CT transverse sections (lower image) and coronal sections (right image) are shown. (B) Radioactivity is significantly increased (P = 0.004, paired t-test) in C19 compared to B9 tumors (n = 3). (C) Examples of dual immunofluorescence staining of TGFβ (green) and pSMAD2 (red) for B9 (top) and C19 (bottom) tumors (n = 3). Nuclei are DAPI counterstained (blue). Compared to B9 tumors, C19 tumors exhibit significantly greater total TGFβ immunoreactivity in arbitrary units (AU) normalized to cell count (t-test, P = 0.03) and pSMAD2 positive cells (t-test, P = 0.03). (D) Cartoon of contralateral LLC (indicated by orange arrow) and (indicated by green arrow) flank tumors bearing mice and ^{89}Zr-fresolimumab PET/CT imaging of mice. (E) Quantification of radioactivity measured in β8 LLC flank tumors was significantly (n = 4, paired t-test, P = 0.004) greater than in LLC tumors. (F) Examples of TGFβ (green) and pSMAD2 (red) dual immunofluorescence staining of LLC (top) and β8 LLC (bottom) tumors. Nuclei are DAPI counterstained (blue). Compared to LLC tumors, β8 LLC tumors (n = 3-5) exhibit significantly greater total TGFβ immunoreactivity normalized to cell count (t-test, P = 0.02) and pSMAD2 positive cells (t-test, P = 0.03). Scale bars indicate 50 μm in C and F.

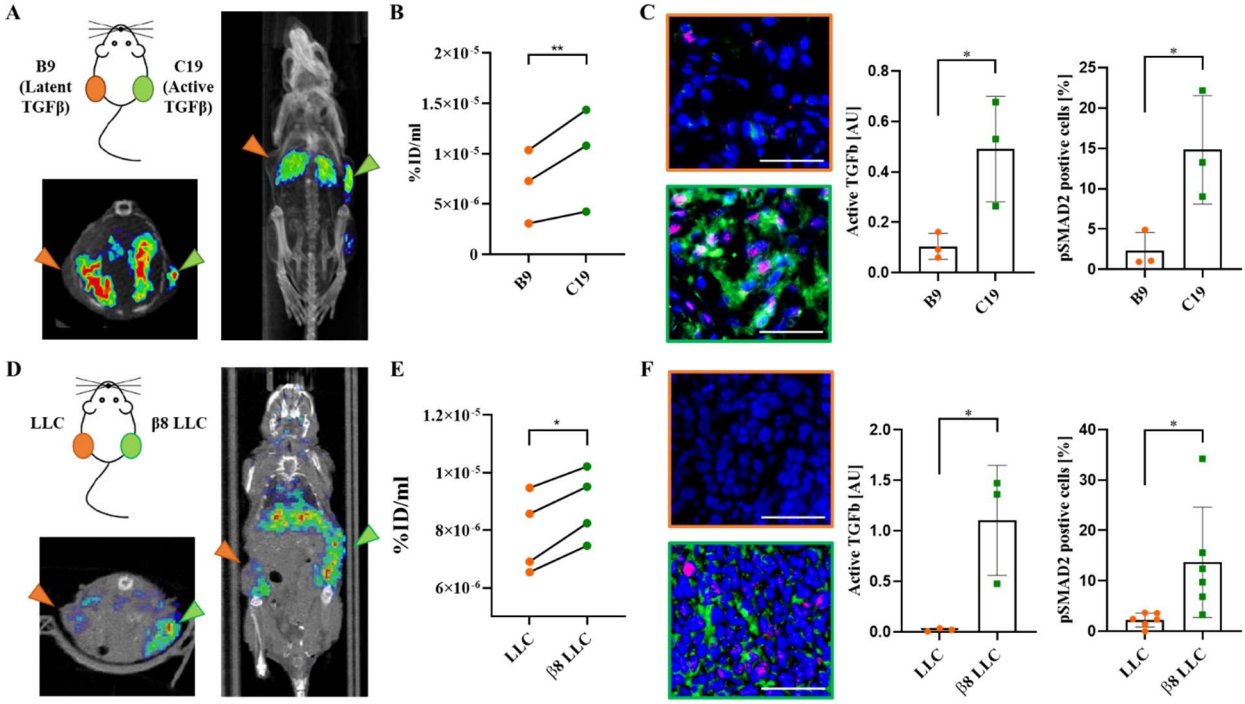

Fig. 2: ^{89}Zr-fresolimumab detects radiation-induced TGFβ activation *in vivo*. (A) ^{89}Zr-fresolimumab PET/CT imaging of 4T1-BrA subcutaneous tumors in which the right flank tumor was irradiated (RT, red arrow) with 15 Gy and the left untreated (sham, blue arrow). (B) Autoradiograms from sham and RT treated tumors ($n = 6$). (C) Radiation significantly ($n = 21$, paired t-test, $P = 0.0002$) increased radioactivity uptake in 4T1-BrA tumors measured *ex vivo* 96 h after ^{89}Zr-fresolimumab injection. (D) The radioactivity of 4T1-BrA tumors from mice injected with unlabeled (cold) fresolimumab significantly decreased (t-test, $P = 0.04$) uptake of labeled ^{89}Zr-fresolimumab (blocked, $n = 6$) compared to ^{89}Zr-fresolimumab (not blocked, $n = 10$) alone. (E) Examples of dual immunofluorescence of active TGFβ (green) and pSMAD2 (red) in 4T1-BrA subcutaneous tumors. DAPI stained nuclei are blue. (F) Quantification of pSMAD2 positive cells from 4T1-BrA subcutaneous tumors (n= 5-7, paired t-test, $P = 0.012$). (G) Distribution of TNC immunofluorescence (red) in 4T1-BrA subcutaneous tumors. DAPI stained nuclei are blue. (H) TNC immunofluorescence was significantly increased in irradiated 4T1-BrA subcutaneous tumors (n= 5-7, t-test, P = 0.008). Scale bars indicate 100 µm in E and G.

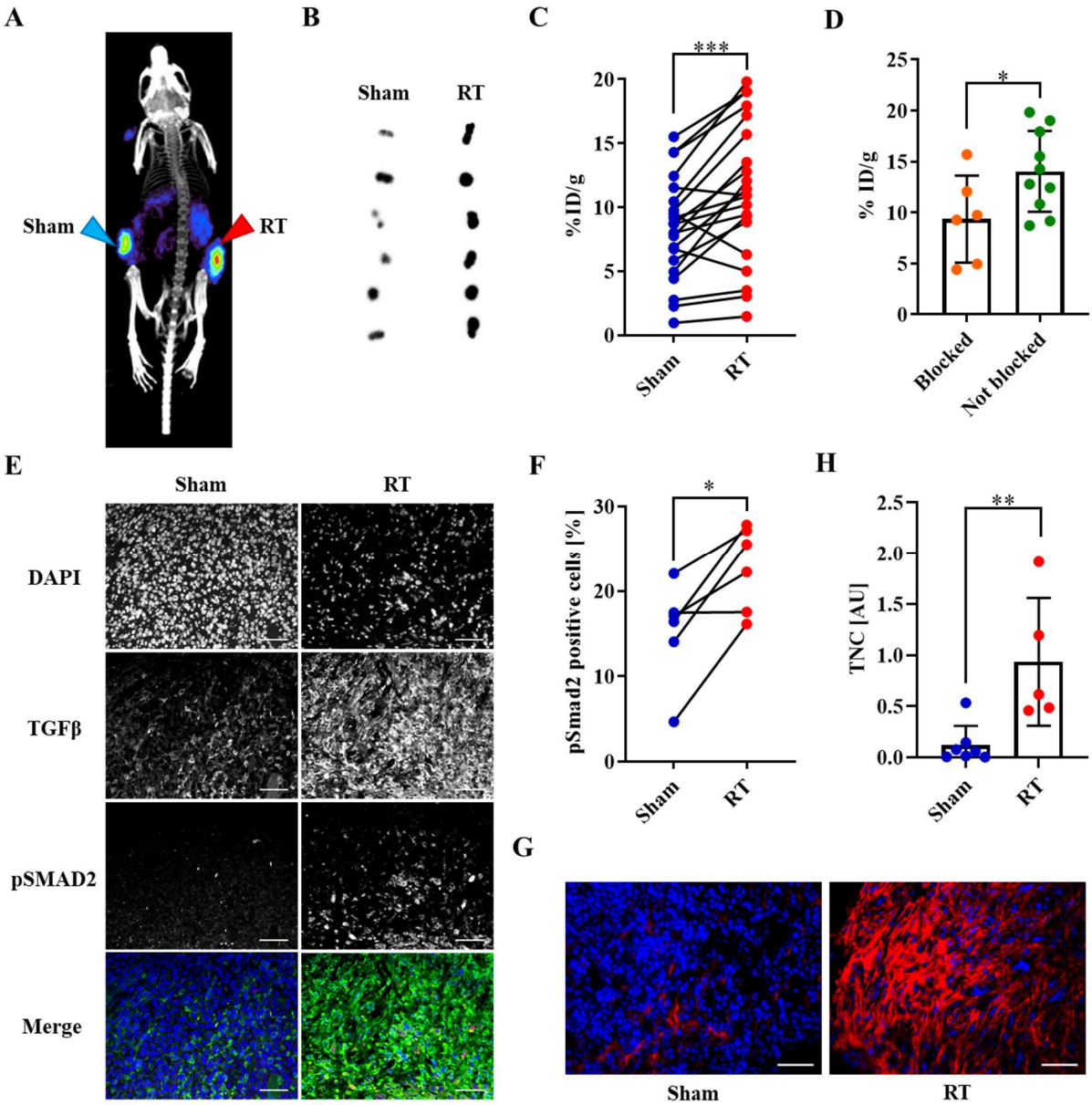

Fig. 3: Detection of TGFβ activity in brain tumors by ^{89}Zr-fresolimumab PET imaging. Coronal (left) and sagittal (middle) images of ^{18}F-FDG PET (upper panel, labeled FDG) and ^{89}Zr-fresolimumab PET (bottom panel, labeled FLM) of mice bearing intracranial (A) SB28, (B) Gl261 and (C) 4T1-BrA tumors imaged with. BLI (right) for each is also shown. (D) Total intracranial radioactivity 120 h after injection in mice bearing SB28 tumors is significantly greater (n = 4, t-test) than PBS injected controls. (E) Total intracranial radioactivity measured by PET 48 h after injection of mice bearing SB28 tumors or GL261 tumors compared to PBS injected controls analyzed (n = 3, t-test). (F) Radioactivity of ^{89}Zr-fresolimumab quantified from PET for mice bearing SB28 or 4T1–BrA intracranial (i.c., n = 5) and subcutaneous (s.c., n = 4) tumors. *P ≤ 0.05, ** P ≤ 0.01, *** P≤0.0001

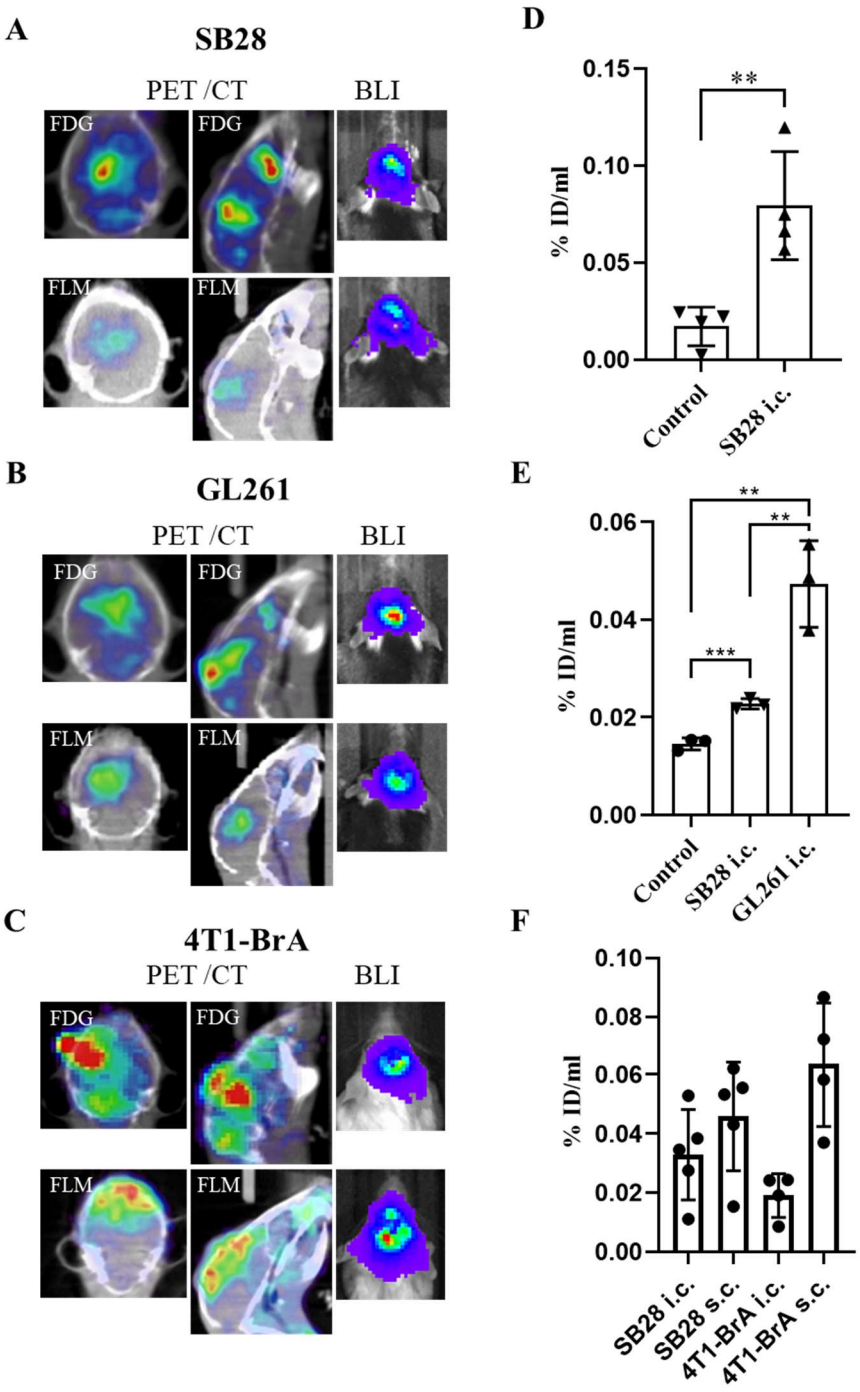

Fig. 4: TGFβ neutralizing antibody 1D11 decreases TGFβ signaling and increases response to RT in intracranial tumors. The percentage of pSMAD2 positive cells was significantly increased (one-way ANOVA) by irradiation and decreased by 1D11 treatment in (A) SB28, (B) GL261 and (C) 4T1-BrA intracranial tumors (n = 3-5). Immunofluorescence of TNC was significantly increased by irradiation and decreased by 1D11 treatment (one-way ANOVA) in (D) SB28, (E) GL261 and (F) 4T1-BrA intracranial tumors (n = 3-5) was significantly increased. (G-I) Kaplan-Meier survival analysis of mice treated with 1D11 (green), RT (orange), combination of both (blue) or control (i.e. sham-irradiated and treated with non-specific IgG, black). RT at day 9 indicated by black arrow. (G) Intracranial SB28 tumors treated with 1D11 (n = 6), RT (n = 9), combination of both (n = 10) or control (n = 9). (H) Intracranial GL261 tumors treated with 1D11 (n = 5), RT (n = 10), combination of both (n = 10) or controls (n = 4). (I) Intracranial 4T1-BrA tumors treated with 1D11 (n = 9), RT (n = 12), combination of both (n = 13) or control (n = 15). *$P \leq 0.05$, ** $P \leq 0.01$, *** P≤0.0001, **** $P \leq 0.0001$